

Istituto  
Nazionale  
Fisica  
Nucleare

Sezione SANITÀ  
Istituto Superiore di Sanità  
Viale Regina Elena 299  
I-00161 Roma, Italy

INFN-ISS 96/8  
September 1996

## Electroproduction of the Roper resonance and the constituent quark model<sup>a</sup>

F. Cardarelli<sup>(1)</sup>, E. Pace<sup>(2)</sup>, G. Salmè<sup>(3)</sup>, S. Simula<sup>(3)</sup>

<sup>(1)</sup> Dept. of Physics and Supercomputer Computations Research Institute  
Florida State University, Tallahassee, FL 32306, USA

<sup>(2)</sup> Dipartimento di Fisica, Università di Roma "Tor Vergata"  
and Istituto Nazionale di Fisica Nucleare, Sezione Tor Vergata  
Via della Ricerca Scientifica 1, I-00133 Roma, Italy

<sup>(3)</sup> Istituto Nazionale di Fisica Nucleare, Sezione Sanità  
Viale Regina Elena 299, I-00161 Roma, Italy

### Abstract

A parameter-free evaluation of the  $N - P_{11}(1440)$  electromagnetic transition form factors is performed within a light-front constituent quark model, using for the first time the eigenfunctions of a mass operator which generates a large amount of configuration mixing in baryon wave functions. A one-body electromagnetic current, which includes the phenomenological constituent quark form factors already determined from an analysis of pion and nucleon experimental data, is adopted. For  $Q^2$  up to few  $(GeV/c)^2$ , at variance with the enhancement found in the elastic channel, the effect of configuration mixing results in a significant suppression of the calculated helicity amplitudes with respect to both relativistic and non-relativistic calculations, based on a simple gaussian-like ansatz for the baryon wave functions.

PACS numbers: 13.60.Rj, 13.40.Gp, 12.39.Ki, 12.39.Pn

---

<sup>a</sup>To appear in *Physics Letters B*.

The investigation of the electromagnetic (e.m.) excitations of nucleon resonances can shed light on their structure in terms of quarks and gluons. In this respect, the Roper resonance,  $P_{11}(1440)$ , plays a particular role. Within the constituent quark ( $CQ$ ) picture (see, e.g., [1, 2]) this resonance is commonly assigned to a radial excitation of the nucleon, whereas it has been argued [3, 4, 5] that it might be a hybrid state, containing an explicit excited glue-field configuration (i.e., a  $q^3G$  state). Within the  $q^3$  assignment the spin-flavour part of the Roper-resonance wave function is commonly considered to be identical to that of the nucleon, whereas the  $q^3G$  state is directly orthogonal to the nucleon in the spin-flavour space. Then, it is expected [4] that such different spin structures of the Roper resonance could lead to different behaviours of its e.m. helicity amplitudes as a function of the four-momentum transfer, so that future experiments planned at  $TJNAF$  [6] might provide signatures for hybrid baryons. However, the predictions of Ref. [4] have been obtained within a non-relativistic framework and using simple gaussian-like wave functions. Within the  $CQ$  model, the relevance of the relativistic effects on the helicity amplitudes of the Roper resonance has been illustrated by Weber [7] and by Capstick and Keister [2], where (we stress) gaussian-like wave functions were still adopted.

The purpose of this letter is to compute the e.m.  $N - P_{11}(1440)$  transition form factors in the relativistic  $CQ$  model developed in [8, 9, 10]. The model incorporates the following features: i) a proper treatment of relativistic effects through the light-front ( $LF$ ) formalism; ii) the use of the eigenfunctions of a baryon mass operator having a much closer connection to the mass spectrum with respect to a gaussian-like ansatz; iii) the use of a one-body approximation for the e.m. current able to reproduce the experimental data on the nucleon form factors. Inside baryons the  $CQ$ 's are assumed to interact via the  $q - q$  potential of Capstick and Isgur ( $CI$ ) [11]. A relevant feature of this interaction is the presence of an effective one-gluon-exchange ( $OGE$ ) term, which produces a huge amount of high-momentum components and  $SU(6)$  breaking terms in the baryon wave functions (see [9, 10]); in what follows we will refer to these effects as the configuration mixing. Finally, an effective one-body e.m. current, including Dirac and Pauli form factors for the  $CQ$ 's (cf. also Ref. [12]), is adopted. The  $CQ$  form factors have been determined in [9] using as constraints the pion and nucleon experimental data. In [10] our parameter-free prediction for the magnetic form factor of the  $N - \Delta(1232)$  transition has been checked against available data. In this letter, our parameter-free results for the  $N - P_{11}(1440)$  helicity amplitudes will be presented, showing that the configuration mixing leads to a significant suppression of the calculated helicity amplitudes with respect to relativistic as well as non-relativistic calculations, based on a simple gaussian-like ansatz for the wave functions.

In the  $LF$  hamiltonian dynamics (cf. [13]) intrinsic momenta of the  $CQ$ 's,  $k_i$ , can be obtained from the on-mass-shell momenta  $p_i$  in a general reference frame, through the  $LF$  boost  $L_f^{-1}(P_0)$ , which transforms the momentum  $P_0 \equiv \sum_{i=1}^3 p_i$  as  $L_f^{-1}(P_0) P_0 = (M_0, 0, 0, 0)$  without Wigner rotations. Thus, one has  $k_i = L_f^{-1}(P_0) p_i$  and, obviously,  $\sum_{i=1}^3 \vec{k}_i = 0$ . In this formalism a baryon state in the  $u - d$  sector,  $|\Psi_{JJ_n}^{TT_3} \pi, \tilde{P}\rangle$ , is an eigenstate of: i) isospin,  $T$  and  $T_3$ ; ii) parity,  $\pi$ ; iii) kinematical (non-interacting)  $LF$  angular momentum operators  $j^2$  and  $j_n$ , where the vector  $\hat{n} = (0, 0, 1)$  defines the spin quantization axis; iv) total  $LF$

baryon momentum  $\vec{P} \equiv (P^+, \vec{P}_\perp) = \vec{p}_1 + \vec{p}_2 + \vec{p}_3$ , where  $P^+ = P^0 + \hat{n} \cdot \vec{P}$  and  $\vec{P}_\perp \cdot \hat{n} = 0$ . We explicitly construct  $|\Psi_{JJ_n \pi}^{TT_3}, \vec{P}\rangle$  as eigenstate of an intrinsic  $LF$  mass operator,  $\mathcal{M} = M_0 + \mathcal{V}$ , where  $M_0 = \sum_{i=1}^3 \sqrt{m_i^2 + \vec{k}_i^2}$  is the free mass operator,  $m_i$  the  $CQ$  mass and  $\mathcal{V}$  a Poincaré invariant interaction. The state  $|\Psi_{JJ_n \pi}^{TT_3}, \vec{P}\rangle$  factorizes into  $|\Psi_{JJ_n \pi}^{TT_3}\rangle |\vec{P}\rangle$  and the intrinsic  $LF$  angular momentum eigenstate  $|\Psi_{JJ_n \pi}^{TT_3}\rangle$  can be constructed from the eigenstate  $|\psi_{JJ_n \pi}^{TT_3}\rangle$  of the *canonical* angular momentum, i.e.  $|\Psi_{JJ_n \pi}^{TT_3}\rangle = \mathcal{R}^\dagger |\psi_{JJ_n \pi}^{TT_3}\rangle$ , by means of the unitary operator  $\mathcal{R}^\dagger = \prod_{j=1}^3 R_{Mel}^\dagger(\vec{k}_j, m_j)$ , with  $R_{Mel}(\vec{k}_j, m_j)$  being the generalized Melosh rotation [13]. One gets

$$(M_0 + V) |\psi_{JJ_n \pi}^{TT_3}\rangle = M |\psi_{JJ_n \pi}^{TT_3}\rangle \quad (1)$$

where  $M$  is the baryon mass. The interaction  $V = \mathcal{R}\mathcal{V}\mathcal{R}^\dagger$  has to be independent of the total momentum  $P$  and invariant upon spatial rotations and translations (cf. [13]). We can identify Eq. (1) with the baryon mass equation proposed by Capstick and Isgur in [11]. The  $CI$  effective interaction  $V = \sum_{i<j} V_{ij}$  is composed by a linear confining term (dominant at large separations) and a  $OGE$  term (dominant at short separations). The latter contains both a central Coulomb-like potential and a spin-dependent part, responsible for the hyperfine splitting of baryon masses. The values  $m_u = m_d = 0.220 \text{ GeV}$  [11] have been adopted throughout this work. As in Refs. [9, 10], the mass equation (1) has been solved by expanding the state  $|\psi_{JJ_n \pi}^{TT_3}\rangle$  onto a (truncated) set of harmonic oscillator ( $HO$ ) basis states and by applying the Rayleigh-Ritz variational principle. We have included in the expansion all the  $HO$  basis states up to 20  $HO$  quanta and the obtained eigenvalues are in agreement with the results of Ref. [11]. The  $S$ ,  $S'$  and  $D$  components have been considered and the corresponding probabilities are:  $P_S^N = 98.1\%$ ,  $P_{S'}^N = 1.7\%$ ,  $P_D^N = 0.2\%$  for the nucleon and  $P_S^{Roper} = 90.6\%$ ,  $P_{S'}^{Roper} = 9.3\%$ ,  $P_D^{Roper} = 0.1\%$  for the Roper resonance. Note that in [14] an approximate treatment of the hyperfine  $OGE$  term led to:  $P_S^{Roper} \simeq 97\%$ ,  $P_{S'}^{Roper} \simeq 3\%$ ,  $P_D^{Roper} \simeq 0.01\%$ . Finally,  $P$  partial waves have been neglected, because they do not couple to the main components of the wave functions.

Let us now consider the  $CQ$  momentum distribution  $n(p)$ , defined as in [10]. The momentum distribution  $n(p)$ , times  $p^2$ , obtained for the nucleon and the Roper resonance using the  $CI$  interaction, is shown in Fig. 1(a) and compared with the gaussian-like ansatz adopted in [2]. It can clearly be seen that the high-momentum tail of both baryon wave functions is sharply enhanced by the effects due to the  $OGE$  interaction. The contributions of the  $S$ ,  $S'$  and  $D$  partial waves to the  $CQ$  momentum distribution are separately shown in Fig. 1(b). It turns out that in case of the Roper resonance the mixed-symmetry  $S'$ -wave, which has a spin-flavour structure orthogonal to that of the symmetric  $S$ -wave component, yields a significant contribution in a wide range of momenta; moreover, for  $p \lesssim 1 \text{ GeV}/c$  the  $S'$  component is much larger in the Roper resonance than in the nucleon. On the contrary, the  $D$ -wave components of both the nucleon and the Roper resonance give a negligible contribution to  $n(p)$ . Therefore, in the calculation of the  $N - P_{11}(1440)$  transition form factors we will neglect the contribution of  $D$ -wave components. The results reported in Fig. 1 clearly show that, when the  $OGE$  interaction is fully considered, the resulting  $CQ$

structure of the Roper resonance contains high radial excitations and sizable mixed-symmetry components, so that it can hardly be interpreted as a simple (first) radial excitation of the nucleon.

The matrix elements of the e.m.  $N - P_{11}(1440)$  transition current can be written as follows (cf., e.g., [7])

$$\begin{aligned} & \langle \Psi_{\frac{1}{2}\nu^*+1}^{\frac{1}{2}\tau^*}, \tilde{P}^* | \mathcal{I}^\mu(0) | \Psi_{\frac{1}{2}\nu+1}^{\frac{1}{2}\tau}, \tilde{P} \rangle = \delta_{\tau^*\tau} \mathcal{I}_{\nu^*\nu}^\mu(\tau) = \\ & \delta_{\tau^*\tau} \bar{u}(\tilde{P}^*, \nu^*) \left\{ F_1^{*\tau}(Q^2) [\gamma^\mu + q^\mu \frac{M^* - M}{Q^2}] + F_2^{*\tau}(Q^2) \frac{i\sigma^{\mu\rho} q_\rho}{M^* + M} \right\} u(\tilde{P}, \nu) \end{aligned} \quad (2)$$

where  $Q^2 \equiv -q \cdot q$  is the squared four-momentum transfer,  $\sigma^{\mu\rho} = \frac{i}{2}[\gamma^\mu, \gamma^\rho]$ ,  $u(\tilde{P}, \nu)$  [ $u(\tilde{P}^*, \nu^*)$ ] the nucleon [Roper-resonance] spinor,  $F_{1(2)}^{*\tau}(Q^2)$  the Dirac (Pauli) form factor associated to the  $N - P_{11}(1440)$  transition and  $\tau = \mp 1/2$  (or  $\tau = n, p$ ). In Eq. (2) the structure  $\gamma^\nu + q^\nu(M^* - M)/Q^2$  is required in order to keep gauge invariance. In the  $LF$  formalism (cf. [13]) the space-like e.m. form factors are related to the matrix elements of the *plus* component of the e.m. current ( $\mathcal{I}^+$ ) and, moreover, the choice  $q^+ = P^{*+} - P^+ = 0$  allows to suppress the contribution of the pair creation from the vacuum [15]. The matrix elements  $\mathcal{I}_{\nu^*\nu}^+(\tau)$  can be cast in the form  $\mathcal{I}_{\nu^*\nu}^+(\tau) = F_1^{*\tau}(Q^2)\delta_{\nu^*\nu} - F_2^{*\tau}(Q^2) i(\sigma_2)_{\nu^*\nu} Q/(M^* + M)$ , where  $\sigma_2$  is a Pauli matrix. Then, the transition form factors  $F_{1(2)}^{*\tau}(Q^2)$  are given by  $F_1^{*\tau}(Q^2) = Tr[\mathcal{I}^+(\tau)]/2$  and  $F_2^{*\tau}(Q^2) = i(M^* + M) Tr[\sigma_2 \mathcal{I}^+(\tau)]/2Q$ .

The  $N - P_{11}(1440)$  transition form factors will be evaluated using the eigenvectors of Eq. (1) and the plus component of the one-body e.m. current of Ref. [9], viz.

$$\mathcal{I}^+(0) = \sum_{j=1}^3 I_j^+(0) = \sum_{j=1}^3 \left( e_j \gamma^+ f_1^j(Q^2) + i\kappa_j \frac{\sigma^{+\rho} q_\rho}{2m_j} f_2^j(Q^2) \right) \quad (3)$$

where  $e_j$  ( $\kappa_j$ ) is the charge (anomalous magnetic moment) of the  $j$ -th quark, and  $f_{1(2)}^j$  its Dirac (Pauli) form factor. Though the full hadron e.m. current has to include two-body components for fulfilling gauge and rotational invariances (see [13]), we have shown [9] that the effective one-body current component (3) is able to give a coherent description of both the pion and nucleon experimental form factors. Moreover, using the  $CQ$  form factors determined in [9], our parameter-free prediction for the magnetic form factor of the  $N - \Delta(1232)$  transition has been checked against available data (see [10]). Let us stress that, since our one-body approximation refers to the  $\mathcal{I}^+$  component of the current only, with a suitable definition of the other components the e.m. current can fulfil gauge invariance.

Our results for the magnetic transition form factor  $G_M^{*p}(Q^2) \equiv F_1^{*p}(Q^2) + F_2^{*p}(Q^2)$ , obtained using the  $CI$  wave functions both with and without the  $CQ$  form factors of Refs. [9, 10], are shown in Fig. 2 for  $Q^2$  up to few  $(GeV/c)^2$  (i.e., in a range of values of  $Q^2$  of interest to  $TJNAF$ ) and compared with the predictions of the relativistic  $q^3$  model of Ref. [2], where a gaussian-like ansatz is adopted for the baryon wave functions and point-like  $CQ$ 's are assumed. As in the case of the elastic  $G_M^p(Q^2)$  form factor (cf. Ref. [9]),  $G_M^{*p}(Q^2)$  is remarkably sensitive to configuration mixing effects. However, for  $Q^2$  up to few  $(GeV/c)^2$  it

turns out that the configuration mixing does not produce in  $G_M^{*p}(Q^2)$  the large enhancement found in the elastic channel. Then, when the  $CQ$  form factor of Ref. [9] are included, our full prediction and the one of Ref. [2] turn out to be quite similar for the proton, but strongly different for the  $p - P_{11}(1440)$  transition. In particular, for  $Q^2 \sim 1 \div 4$  ( $GeV/c$ )<sup>2</sup> our magnetic form factor  $G_M^{*p}(Q^2)$  is suppressed with respect to the prediction of Ref. [2] by a large factor ( $\sim 3 \div 4$ ), which implies a reduction of about one order of magnitude for the electroproduction cross section of the Roper resonance.

In what follows, our results will be shown in terms of the helicity amplitudes  $A_{\frac{1}{2}}^\tau(Q^2)$  and  $S_{\frac{1}{2}}^\tau(Q^2)$ , defined as

$$A_{\frac{1}{2}}^\tau(Q^2) = \mathcal{N}(Q^2) G_M^{*\tau}(Q^2) \quad , \quad S_{\frac{1}{2}}^\tau(Q^2) = \mathcal{N}(Q^2) \frac{\sqrt{2K^-K^+} M^* + M}{Q^2} \frac{M^* + M}{4M^*} G_E^{*\tau}(Q^2) \quad (4)$$

where  $\mathcal{N} \equiv \sqrt{\frac{\pi\alpha}{K^*} \frac{K^-}{M^*M}}$ ,  $K^\pm \equiv Q^2 + (M^* \pm M)^2$ ,  $K^* \equiv (M^{*2} - M^2)/2M^*$  and  $G_E^{*\tau} \equiv F_1^{*\tau} - Q^2 F_2^{*\tau}/(M^* + M)^2$ . Our parameter-free predictions for  $A_{\frac{1}{2}}^{p(n)}(Q^2)$  and  $-S_{\frac{1}{2}}^{p(n)}(Q^2)$  are shown in Fig. 3 and compared with the photoproduction values [16] and the results of phenomenological analyses [17, 18] of available electroproduction data, as well as with the predictions of the relativistic  $q^3$  model of Ref. [2] and of the non-relativistic  $q^3$  and  $q^3G$  models of Ref. [4](c). Moreover, in order to better illustrate the effects of the configuration mixing, the result obtained excluding the  $S'$  component of the  $CI$  wave functions of both the nucleon and the Roper resonance, is also reported in Fig. 3. As in case of  $G_M^{*p}(Q^2)$ , our results both for the transverse  $A_{\frac{1}{2}}^{p(n)}(Q^2)$  and the longitudinal  $S_{\frac{1}{2}}^{p(n)}(Q^2)$  helicity amplitudes exhibit a remarkable reduction with respect to non-relativistic as well as relativistic predictions, based on simple gaussian-like wave functions. Such a reduction brings our predictions closer to the results of the phenomenological analyses of Refs. [17, 18]<sup>b</sup>. At the photon point it can be seen that: i) our prediction for  $A_{\frac{1}{2}}^n(Q^2 = 0)$  agrees well with the *PDG* value [16], while the absolute value of  $A_{\frac{1}{2}}^p(Q^2 = 0)$  is underestimated; ii) the longitudinal helicity amplitudes  $S_{\frac{1}{2}}^p(Q^2 = 0)$  and  $S_{\frac{1}{2}}^n(Q^2 = 0)$  are remarkably sensitive to the presence of the mixed-symmetry  $S'$  component in the  $CI$  wave functions. The latter feature holds as well up to  $Q^2 \sim \text{few } (GeV/c)^2$ , whereas the transverse helicity amplitudes  $A_{\frac{1}{2}}^{p(n)}(Q^2)$  are only slightly modified by the  $S'$  partial waves. Finally, it turns out that the relativistic predictions of the ratio  $A_{\frac{1}{2}}^n(Q^2)/A_{\frac{1}{2}}^p(Q^2)$  differ remarkably from the non-relativistic result of the  $q^3$  and  $q^3G$  models (i.e.,  $A_{\frac{1}{2}}^n(Q^2)/A_{\frac{1}{2}}^p(Q^2) = -2/3$ ). This result, which is clearly crucial in a comparison with experimental data, is mainly due to  $S'$  components and to kinematical relativistic effects associated to the Melosh rotations; in particular, at the photon point we obtain:  $A_{\frac{1}{2}}^n/A_{\frac{1}{2}}^p \simeq -4/3$  and  $\simeq -1.1$  with and without the  $S'$  components, respectively.

Recently [4](c), it has been argued that the uncertainties related to the lack of a precise knowledge of the baryon wave functions might cancel out in the ratio between transverse and

---

<sup>b</sup>It should be reminded that model-dependent assumptions made in Refs. [17, 18] might produce significant uncertainties in the data analyses.

longitudinal helicity amplitudes. Thus, in order to check this point, our predictions for the ratio  $A_{\frac{1}{2}}^p(Q^2)/[-S_{\frac{1}{2}}^p(Q^2)]$  are shown in Fig. 4 and compared with the results of non-relativistic [4](c) and relativistic [2] calculations, based on a simple gaussian-like ansatz for the baryon wave functions. It can clearly be seen that up to  $Q^2 \sim 2 (GeV/c)^2$  the ratio exhibits a small sensitivity to configuration mixing effects as well as to the e.m. structure of the  $CQ$ 's, whereas it is strongly modified by relativistic effects. In this respect we want to stress that the relevance of the effects due to the relativistic compositions of the  $CQ$  spins, firstly shown in [7] and clearly exhibited in Figs. 3 and 4, suggests that these effects, as well as those arising from the configuration mixing, should be fully included in the predictions of the hybrid  $q^3G$  model, before a meaningful comparison with our light-front  $CQ$  picture can be performed. Finally, note that for  $Q^2 \sim 0.2 \div 0.6 (GeV/c)^2$  the relativistic predictions of the transverse amplitudes change sign, independently of the effects from the configuration mixing and the  $CQ$  form factors; therefore, for  $Q^2 \sim 0.2 \div 0.6 (GeV/c)^2$  the Roper-resonance production cross section is expected to be mainly governed by its longitudinal helicity amplitude.

In conclusion, the  $N - P_{11}(1440)$  electromagnetic transition form factors have been analyzed within a light-front constituent quark model, using for the first time baryon wave functions, which incorporate the configuration mixing generated by the effective one-gluon-exchange potential of Ref. [11], and a one-body electromagnetic current, which includes the phenomenological constituent quark form factors determined in [9] from an analysis of pion and nucleon experimental data. It has been shown that the effects of the configuration mixing (i.e., high-momentum components and  $SU(6)$  breaking terms) in the Roper-resonance wave function are large and prevent to consider the structure of this resonance as a simple (first) radial excitation of the nucleon. It has been found that the configuration mixing yields a remarkable suppression of the calculated helicity amplitudes with respect to relativistic and non-relativistic predictions, based on a simple gaussian-like ansatz for the baryon wave functions. Moreover, the longitudinal helicity amplitudes exhibit an appreciable sensitivity to the mixed-symmetry  $S'$  components, generated in the baryon wave functions by the hyperfine interaction.

**Acknowledgments.** One of the authors (F.C.) acknowledges the partial support by the U.S. DOE through Contract DE-FG05-86ER40273, and by the SCRI of the Florida State University, partially funded through the Contract DE-FC05-85ER250000.

## References

- [1] R. Koniuk and N. Isgur: Phys. Rev. **D21** (1980) 1868.
- [2] S. Capstick and B. Keister: Phys. Rev. **D 51** (1995) 3598.
- [3] T. Barnes and F.E. Close: Phys. Lett. **B123** (1983) 89; *ib.* **B128** (1983) 277.
- [4] (a) Z. Li and F.E. Close: Phys. Rev. **D42** (1990) 2207. (b) Z. Li: Phys. Rev. **D44** (1991) 2841. (c) Z. Li, V. Burkert and Z. Li: Phys. Rev. **D46** (1992) 70.

- [5] C.E. Carlson and N.C. Mukhopadhyay: Phys. Rev. Lett. **67** (1991) 3745.
- [6] TJNAF proposals: 89-038, spokespersons V.D. Burkert, M. Gai and R. Minehart; 91-002, spokespersons P. Stoler, V.D. Burkert and M. Taiuti; 93-036, spokespersons R. Chasteler, R. Minehart and H. Weller. See, also, V.D. Burkert: AIP Conf. Proc. **334** (1995) 127, ed. by F. Gross.
- [7] H.J. Weber: Phys. Rev. **C41** (1990) 2783.
- [8] F. Cardarelli et al.: Phys. Lett. **332B** (1994) 1; Phys. Rev. **D53** (1996) 6682; Phys. Lett. **B349** (1995) 393; Phys. Lett. **B359** (1995) 1; Few-Body Syst. Suppl. **9** (1995) 267.
- [9] F. Cardarelli, E. Pace, G. Salmè and S. Simula: Phys. Lett. **B357** (1995) 267; Few-Body Syst. Suppl. **8** (1995) 345.
- [10] F. Cardarelli, E. Pace, G. Salmè and S. Simula: Phys. Lett. **B371** (1996) 7.
- [11] S. Capstick and N. Isgur, Phys. Rev. **D 34** (1986) 2809.
- [12] S. Foster and G. Hughes, Z. Phys. **C14** (1982) 123; Rep. Prog. Theor. Phys. **46** (1983) 1445.
- [13] B.D. Keister and W.N. Polyzou, Adv. in Nucl. Phys. **20** (1991) 225. F. Coester, Prog. in Part. and Nucl. Phys. **29** (1992) 1.
- [14] N. Isgur and G. Karl: Phys. Rev. **D19** (1979) 2653.
- [15] L. Frankfurt and M. Strikman, Nucl. Phys. **B 148** (1979) 107. G.P. Lepage and S.J. Brodsky, Phys. Rev. **D 22** (1980) 2157.
- [16] Particle Data Group, R.M. Barnett et al.: Phys. Rev. **D54** (1996) 1.
- [17] C. Gerhardt: Z. Phys. **C4** (1980) 311.
- [18] B. Boden and G. Krosen: in Proc. of the Conf. on *Research Program at CEBAF II*, ed. by V. Burkert et al., CEBAF (USA), 1986.

## Figure Captions

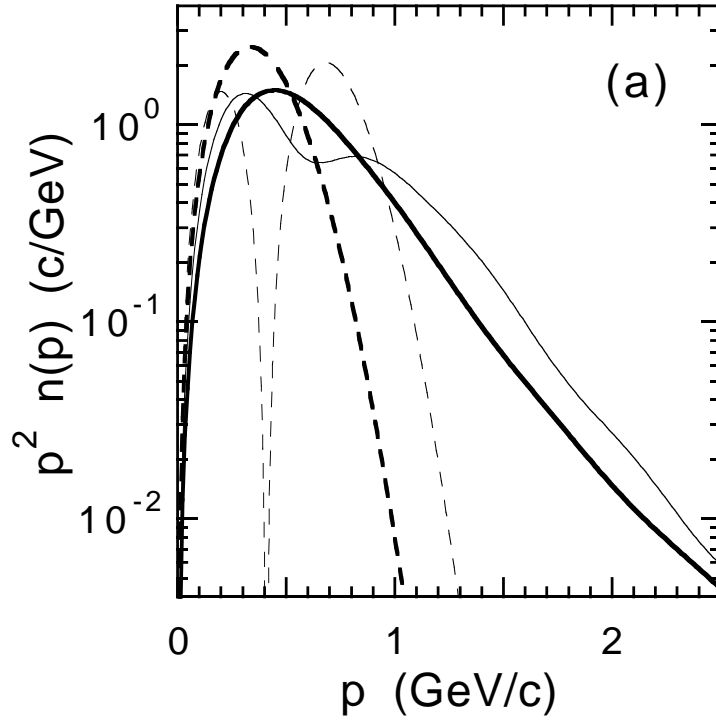
Fig. 1. (a) The momentum distribution  $n(p)$  of the constituent quarks in the nucleon (thick lines) and in the Roper resonance (thin lines), times  $p^2$ . The solid and dashed lines are the  $CQ$  momentum distributions obtained from the eigenstates of Eq. (1) with the  $CI$  interaction [11] and those corresponding to the gaussian-like ansatz, adopted in [2], respectively. (b) Contributions of various partial waves to the  $CQ$  momentum distribution (times  $p^2$ ) in the nucleon (thick lines) and in the Roper resonance (thin lines), obtained using the  $CI$  interaction. The solid, dashed and dot-dashed lines correspond to the  $S$ ,  $S'$  and  $D$  partial-wave contributions, respectively.

Fig. 2. The magnetic form factor  $G_M^{*p}(Q^2)$  for the  $p - P_{11}(1440)$  transition versus  $Q^2$ . The solid line is our prediction, obtained using the eigenstates of the mass equation (1) with the  $CI$  interaction and the one-body current component (3) with the  $CQ$  form factors of Ref. [9]. The dotted line is obtained with the  $CI$  wave functions, but assuming point-like  $CQ$ 's (i.e., putting in Eq. (3)  $f_1^j = 1$  and  $\kappa_j = 0$ ). The dot-dashed line is the result of Ref. [2], obtained using a simple gaussian-like ansatz for the baryon wave functions and assuming point-like  $CQ$ 's.

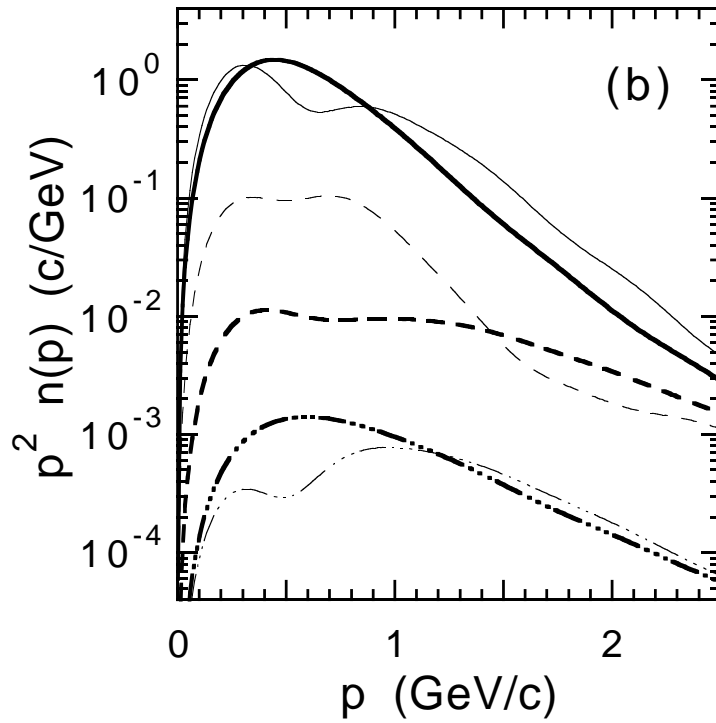
Fig. 3. The  $N - P_{11}(1440)$  helicity amplitudes  $A_{\frac{1}{2}}^{p(n)}(Q^2)$  and  $-S_{\frac{1}{2}}^{p(n)}(Q^2)$ , as a function of  $Q^2$ . The full dots are the  $PDG$  values [16], while the full squares and open dots are the results of the analysis of available electroproduction data performed in Refs. [17] and [18], respectively. Thick lines correspond to the results of  $LF$  calculations. The solid and dot-dashed lines are the same as in Fig. 2. The dashed lines are the results of our calculations performed excluding the  $S'$ -wave components of the  $CI$  wave functions of both the nucleon and the Roper resonance. Thin lines are the results of non-relativistic calculations of Ref. [4](c). The long-dashed and dot-dashed lines correspond to the  $q^3G$  and  $q^3$  models, evaluated using Eqs. (5) and (8) of Ref. [4](c), respectively. Note that within the hybrid  $q^3G$  model  $S_{\frac{1}{2}}^{p(n)}(Q^2) = 0$ , whereas only  $S_{\frac{1}{2}}^n(Q^2)$  is vanishing within the non-relativistic  $q^3$  model. In (b) and (d) the error bars on the solid thick line represent the uncertainties related to the numerical Monte Carlo integration procedure.

Fig. 4. Ratio of the transverse  $A_{\frac{1}{2}}^p(Q^2)$  to the longitudinal  $-S_{\frac{1}{2}}^p(Q^2)$  helicity amplitudes of the  $p - P_{11}(1440)$  transition, as a function of  $Q^2$ . Thick lines correspond to the results of  $LF$  calculations. The solid, dashed, dotted and dot-dashed lines are the same as in Figs. 2 and 3. The thin dot-dashed line is the prediction of the non-relativistic  $q^3$  model of Ref. [4](c). The errors bars are as in Fig. 3.

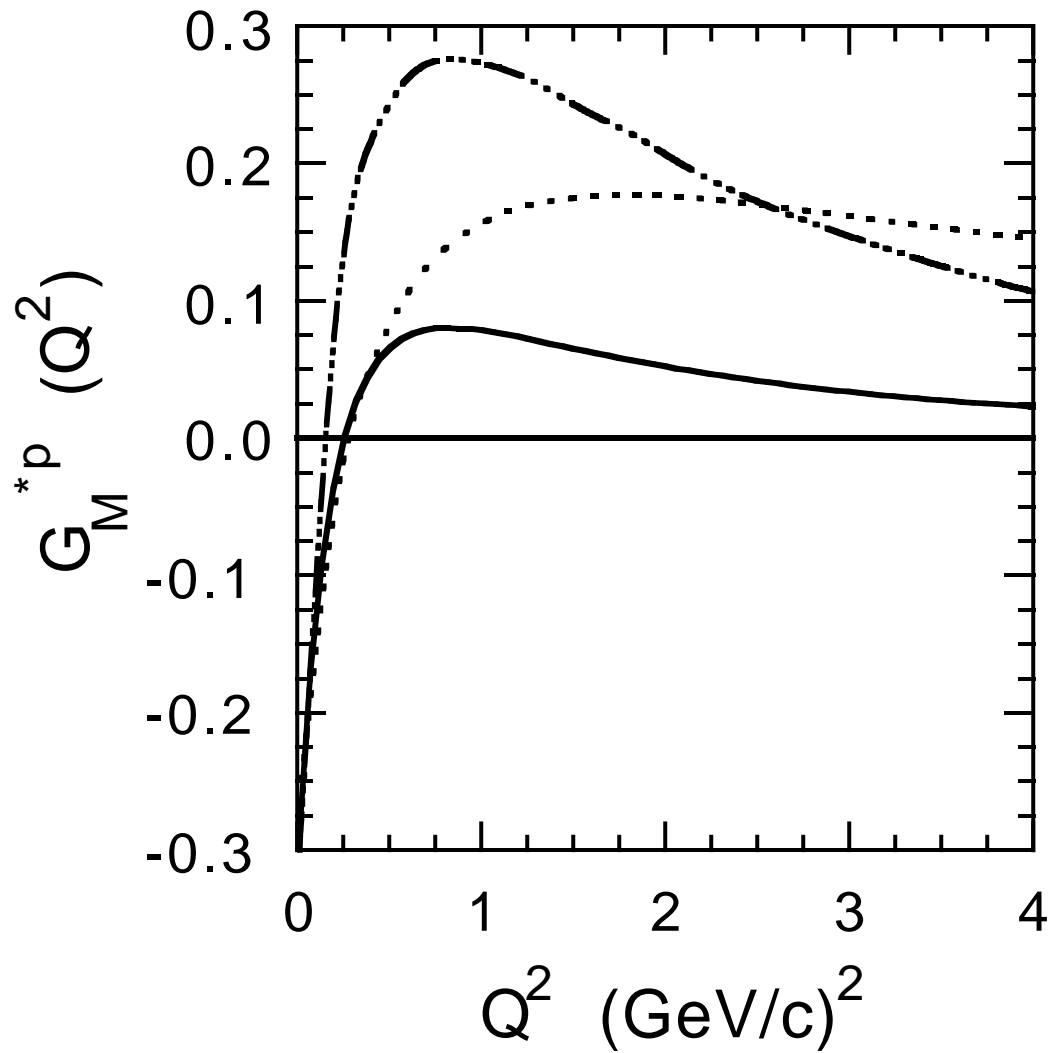




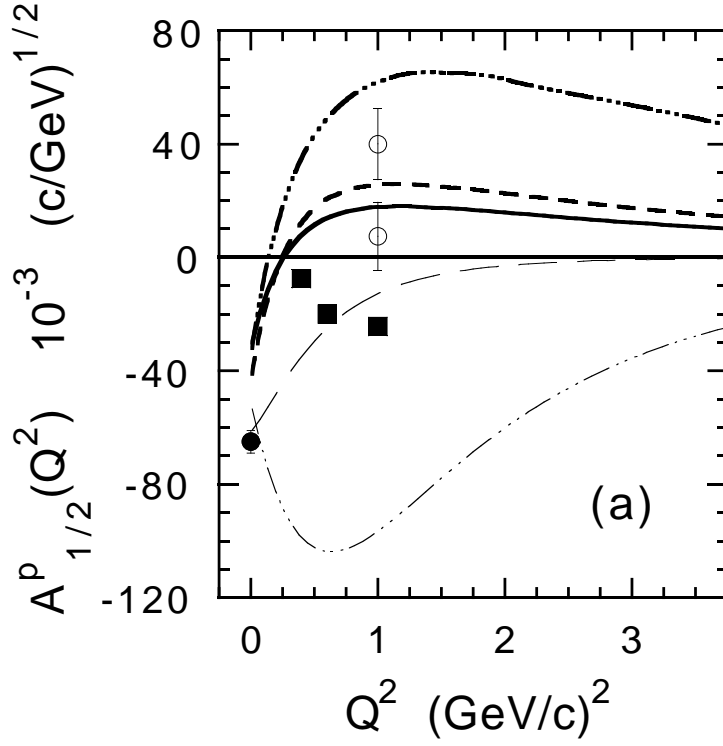
F. Cardarelli, E. Pace, G. Salmè, S. Simula, Phys. Lett. B: fig. 1a



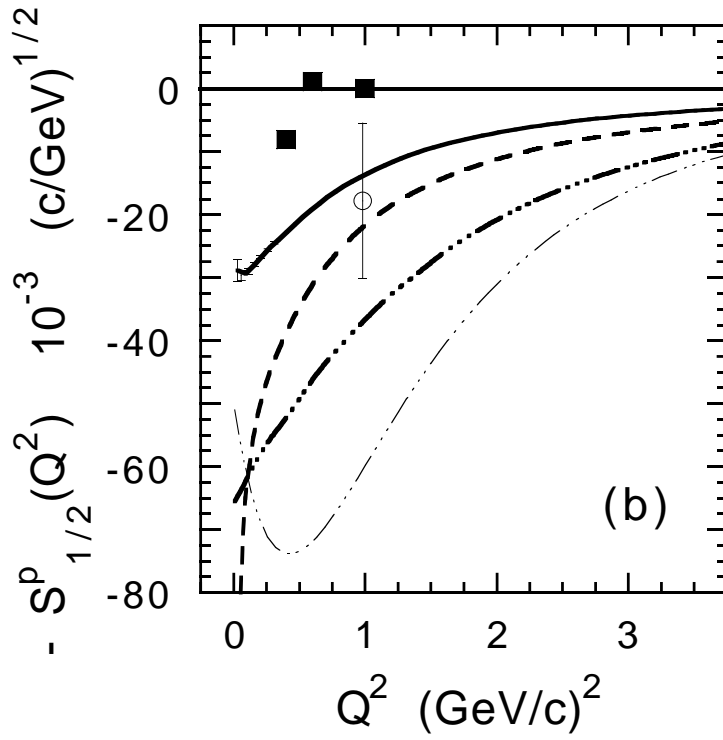
F. Cardarelli, E. Pace, G. Salmè, S. Simula, Phys. Lett. B: fig. 1b



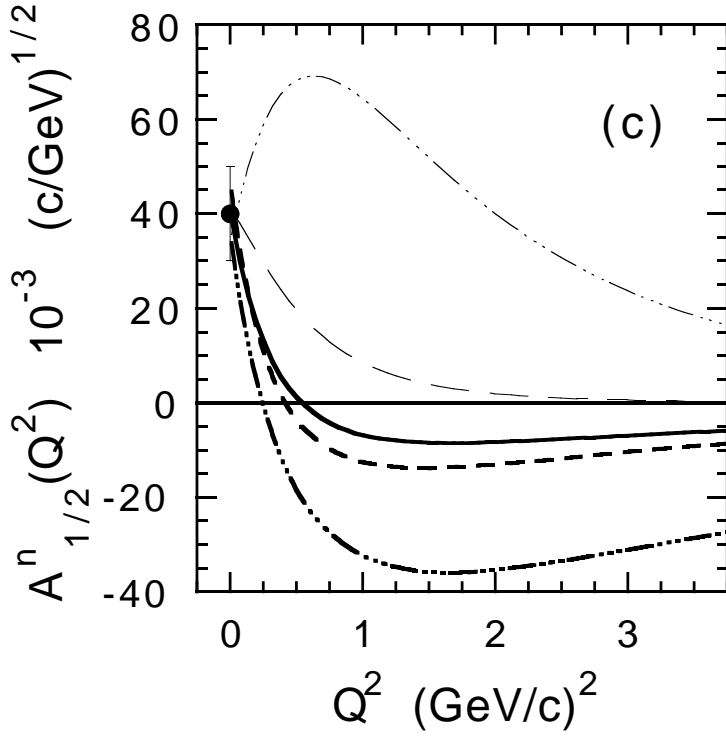
F. Cardarelli, E. Pace, G. Salmè, S. Simula, Phys. Lett. B: fig. 2



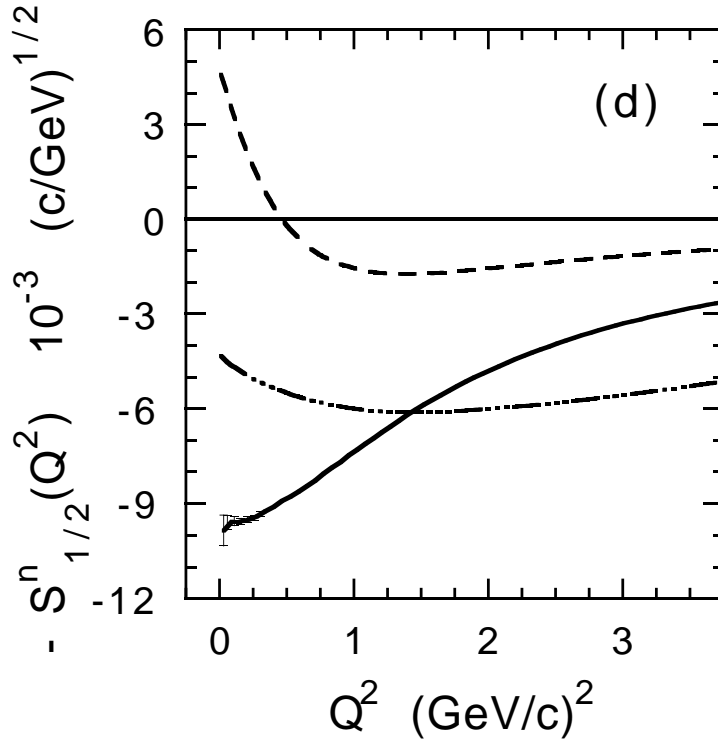
F. Cardarelli, E. Pace, G. Salmè, S. Simula, Phys. Lett. B: fig. 3a



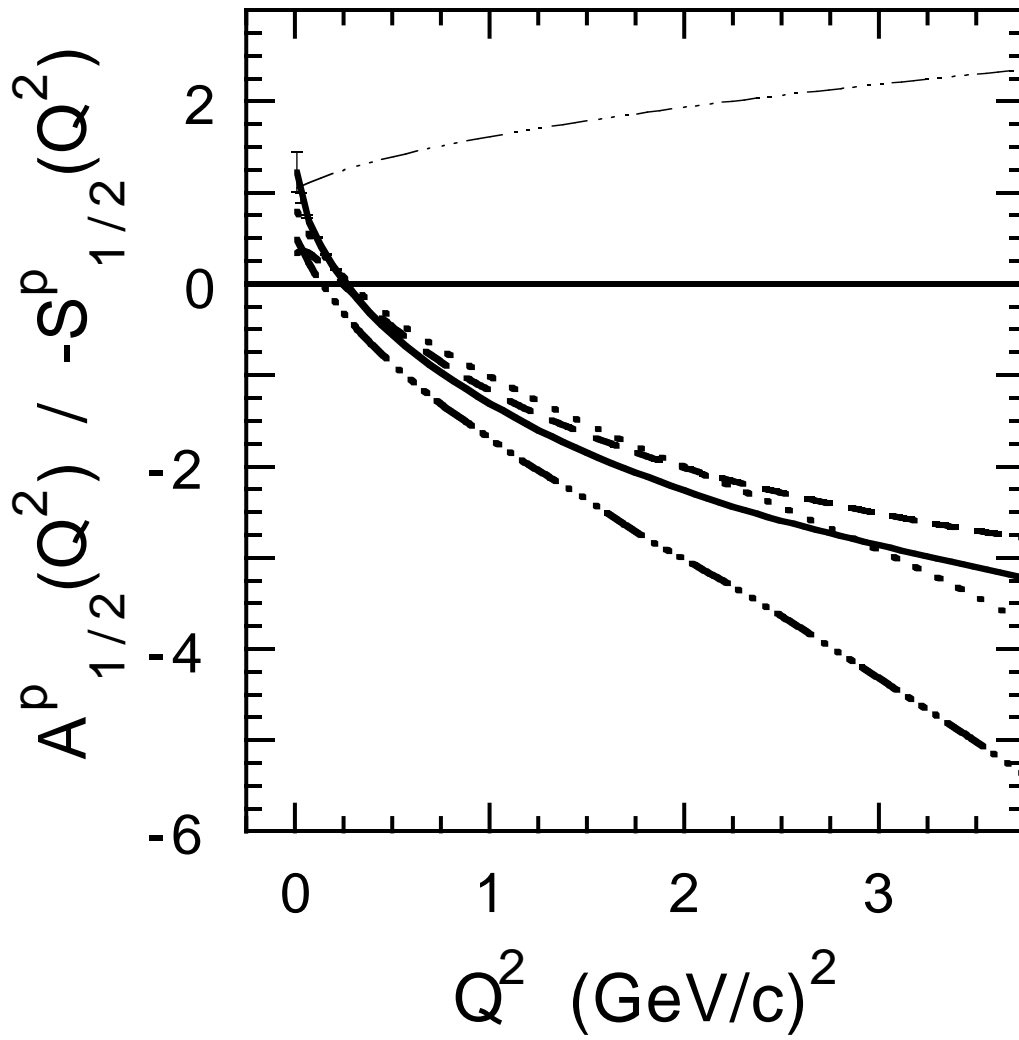
F. Cardarelli, E. Pace, G. Salmè, S. Simula, Phys. Lett. B: fig. 3b



F. Cardarelli, E. Pace, G. Salmè, S. Simula, Phys. Lett. B: fig. 3c



F. Cardarelli, E. Pace, G. Salmè, S. Simula, Phys. Lett. B: fig. 3d



F. Cardarelli, E. Pace, G. Salmè, S. Simula, Phys. Lett. B: fig. 4